JOURNAL OF MATERIALS SCIENCE 25 (1990) 2743–2753

Structure and wear resistance of Ti and TiAl surfaces implanted with B, C, N, O

J. C. PIVIN
C.S.N.S.M. Bâtiment 108, Campus Universitaire, 91405 Orsay, France

The composition and the structure of as-implanted and of worn surfaces were determined by means of several spectroscopies (RBS, NRA and SIMS) and of transmission electron microscopy (TEM). The structural transformations during implantation were often different to those previously reported and new compounds were obtained. The main factor of wear for all films was a local cracking induced by the sinking of a more plastic substrate. When the latter was pure Ti, oxygen diffusion through these cracks and adhesion between stripped areas of Ti and the friction counterpart enhanced the wear process. The contamination of Ti nitrides with O either during implantation or friction appeared also as another important parameter contributing to lessen their wear resistance. Otherwise the kinetics were in the ratio of films hardnesses.

1. Introduction

Among the large variety of chemically vapour deposited (CVD) and physically vapour deposited (PVD) coatings containing C, N, O developed over ten years, TiC and TiN are commonly used in technological applications requiring a high hardness and conductivity. They are now replaced by carbides and nitrides of Ti and Al which are harder and less oxidable (a maximum hardness is attained for a ratio of concentrations $C_{Al}/C_{Ti} = 1/2$ and $C_C/C_N = 1/7$, correlated to a optimum number of 8.5 valence electrons in such compounds [1, 2]. On the other hand it is well known that oxide coatings are softer but provide the surface a lower friction coefficient [3, 4]. The properties of borides were less studied but it has been suggested [5] that they could exhibit simultaneously a higher hardness and ductility than TiN because of their tendency to amorphicity. They would also be more adherent to the Ti substrate [1] and develop a protective B_2O_3 film during friction.

Now the commonly received idea that implantation films are more adherent than other coatings, because their interface with the substrate is generally diffuse, has led several authors to compare the wear resistance of TiC, TiN, TiB_2 films obtained by this technique or by vapour deposition [6–8]. It has been shown that ion implantation can be more efficient than gas nitriding in not too severe loading conditions, when combined with a thermal treatment providing the film with a particular structure [6]. The respective wear resistances of TiC, TiN and TiB_2 implantation films are subject to discussion [7–10]. Indeed they depend strongly on the ratio of the film and substrate hardnesses. An improvement 10 to 30 times higher has been observed for C implanted in the alloy Ti Al 6% V 4% (as compared with similar concentrations of N, B implanted on the same range of depth) [7–9]. On the contrary other authors have found that C and N were equally effective in hardening and improving the abrasion resistance of pure Ti, but that C did not change the wear kinetics of Ti Al 6% V 4% [10]. Note that the friction conditions of these various studies were very different and that the actual composition and structure of films has not always been checked. Particularly a contamination with a few per cents of C or O modifies drastically the structure of $Ti_{1-x}N_x$ films [11–14]. It induces the precipitation of the cubic δ-TiN nitride even at low N contents instead of the formation of α-$Ti_{1-x}N_x$ solid solutions (for atomic concentrations x in the range 0 to 15%) and of ε-Ti_2N (for x in the range 15 to 30%), expected on basis of the phase diagram. Similarly, either the orthorhombic boride TiB or an amorphous compound, then the hexagonal boride TiB_2 at higher concentrations, can be obtained according to implantation conditions [7, 8, 15, 16].

The present study is a synthesis of previously published data on Ti implanted with N and of new results on the structure and wear resistance of Ti, Ti Al implanted with N, C, B, N + O. These double implantations were expected to produce films combining the lubricant character of oxides and the hardness of nitrides. The structure of films has been determined by TEM and their wear mechanism has been investigated on basis of depth profiles of composition, by means of Rutherford Backscattering Spectrometry (RBS), Nuclear Reactions Analysis (NRA) and Secondary Ion Mass Spectrometry (SIMS).

2. Experimental procedure

Pure Ti and Al (Material Research "Marz" grade with less than 0.2% impurities) were melt together under a vacuum of 10^{-7} torr in order to obtain alloys of compositions Ti 50% Al 50% and Ti 66% Al 34% (checked by electron microprobe analysis). The second one was very brittle and exhibited a lot of cracks. However the few results on the structure of

0022–2461/90 $03.00 + .12

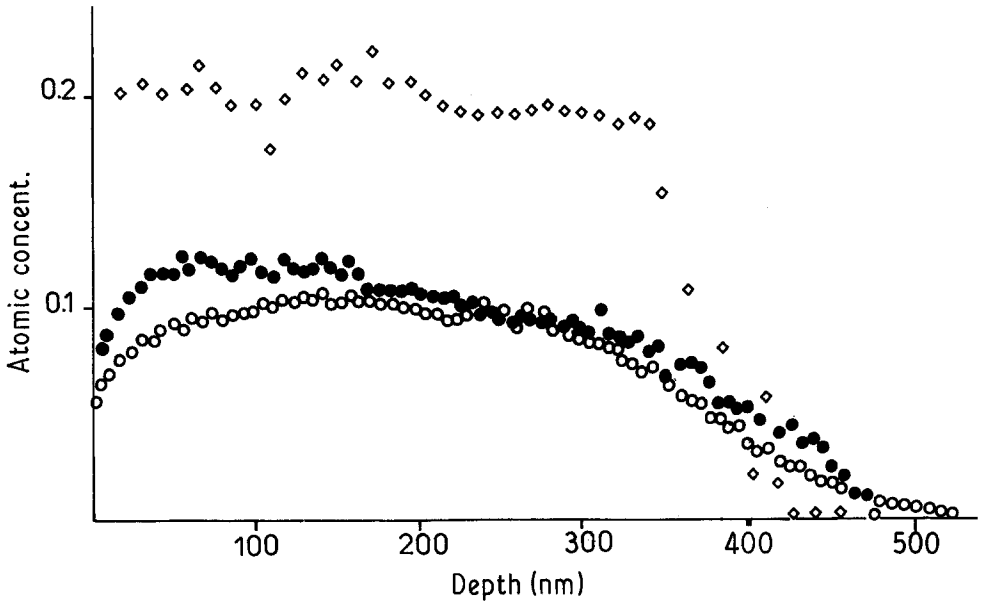

Figure 1 Depth profiles of (●) C 18_0, (○) C 15_N, (◇) 1-C_{Ti} in titanium implanted with 2.4×10^{17} N and 2.4×10^{17} O per cm^2.

implantation films in this alloy will be presented because of the difference in the structure of the two ingots. An hexagonal Ti_2Al phase was identified by X-ray diffraction in the case of Ti 66% Al 34%, while the Ti 50% Al 50% alloy was mainly constituted of the TiAl cubic phase (with a strong (1 1 1) texture) and a few inclusions of Ti_2Al. Metallographic observations have shown that they were randomly distributed in the matrix and their size was about 1 micrometer.

The surface of all Ti, TiAl, Ti_2Al specimens has been polished electrolytically in the Blackburn bath, then they have been implanted in the C.S.N.S.M. machine. The ionic current was always kept lower than 10 $\mu A\,cm^{-2}$ and the residual pressure around the targets lower than 10^{-7} torr in order to avoid any significant heating and contamination of implantation films. Ions were implanted successively at five energies of 190, 145, 80, 50 and 20 keV with fluences in the ratio 1,0.7,0.7,0.4,0.3, chosen on basis of previous experiments [13]. The resulting films of thickness in the range 350 to 400 nm (depending on their concentration) have an homogeneous composition, as shown by Fig. 1.

Such depth profiles of composition could be determined by NRA only for samples implanted with ^{15}N or ^{18}O isotopes. The nuclear reactions $^{15}N(p,\alpha\gamma)^{12}C$ and $^{18}O(p,\alpha)^{15}N$ exhibit sharp resonances at E_R = 898 keV and $E_{R'}$ = 629 keV respectively, i.e. the cross sections of these reactions exhibit intense peaks of width 2.5 keV around these energies. Depth profiles are obtained by increasing the energy E of incoming protons step by step, such that the resonance occurs at a depth where they have loss the energy excess $(E-E_R)$ or $(E-E_{R'})$. These experiments are detailed in [17], as also the procedure used for depth profiling any implanted species by RBS on atoms of the host metal. Indeed, one cannot generally detect light elements in a heavier matrix by this technique because the scattering cross-section of probing particles (generally α ions) varies as Z^2. Thus for most RBS experiments performed with the 2 MV Van de Graff accelerator of the GPS in Paris, the metalloid concentration was taken as the complement to 100% of the Ti one. In the case of implanted specimens such profiles are reliable (Fig. 1). The high plateau of the carbon cross section between 5.5 and 5.7 MeV, due to a nuclear contribution to scattering [18], permitted us to profile directly the concentration of this element (experiments with a He^{++} beam provided by the 4 MV accelerator of IPN in Lyon). The global numbers of C, N O per unit area of the target have been measured by means of non-resonant (d, p) nuclear reactions. Reactions on B were not usable because of their in-energy width and of their low yield requiring the use of a very large detector [19]. A complementary analysis by SIMS permitted the acquisition of less quantitative but systematic profiles for all elements in any target (especially TiB, TiAlB).

The structure of the compounds formed for increasing fluences was investigated *in situ* during implantation in the case of Ti implanted with ^{14}N or ^{11}B, using the electron microscope on line with the implantor (under a vacuum better than 10^{-8} torr (see [20] for experimental details)). At first such experiments did not appear useful in the case of ^{12}C and ^{16}O implantations since the only known phases obtained by ion implantation (or another process in the case of C) are the δ-TiC or δ-TiO compounds, with a cubic structure of the NaCl type. TiC precipitates in the Ti lattice for C concentrations over 1%, and TiO for O concentrations over 32%. Thus the structure of Ti implanted with C or O+N, or of TiAl implanted with 50% of any species was only checked by TEM on samples electrolytically thinned from the unimplanted side. On the contrary, structural changes were investigated *in situ* for Ti_2Al implanted with N because a Ti_2AlN compound, being more ductile than δ-Ti_2AlN_3, could form at intermediate fluences.

These various experiments could be performed not only on as-implanted samples but also after wear tests. Indeed the used tribomoter was specially conceived to generate homogeneous wear tracks of several mm^2, by

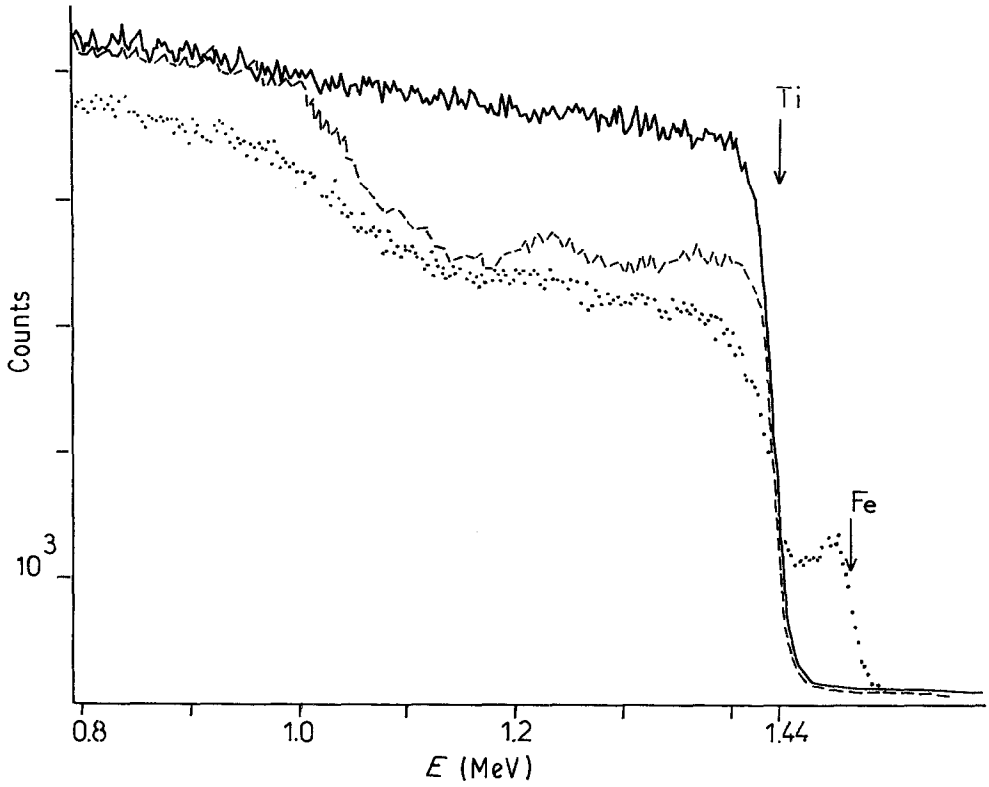

Figure 2 RBS spectra recorded on pure Ti (——), Ti as implanted with 1.7×10^{18} B $\times$ cm^{-2} (– – –) and after a friction test against steel of 500 scans under a pressure of 0.7 GPa (• •). The arrows show the threshold energies of backscattering by Fe and Ti atoms for 2 MeV α particles.

giving the friction counterpart a scanning motion [17]. In the present case the implanted surfaces were rubbed against balls of a 100C6 steel (H_v = 0.8 GPa). A few tests were also performed with ruby (H_v = 1.7 GPa) and TiN (H_v = 20 GPa) riders. The contact pressure was varied by increasing the load (0.05 to 1 N) and the radius of the balls (1 to 10 mm). If one assumes that the contact remained Hertzian in order to give a crude estimation of the pressure, it ranged between 0.1 and 1.5 GPa. The contact area being wider than 50 μm under the lowest pressure, the chosen scanning motion was composed of repeated (60 times) translations of 3 mm in one direction, then 50 μm in the perpendicular direction, such that tracks overlap and a squared area was worn homogeneously.

The usefulness of analyzing the composition of wear tracks by means of several techniques is shown by Fig. 2. The interpretation of RBS spectra was not straightforward. First, when the implanted specimen was rubbed against steel there was often an iron transfer on its surface. However the titanium profile was not distorted because the amount of iron corresponded generally to a surface coverage lower than 10%. The decrease of Ti concentration measured at energies between 0.8 and 1.4 MeV on Fig. 2 is due to a contamination with oxygen and carbon. The gradient of the sum of metalloid concentrations one would deduce from such a spectrum might be interpreted as being due to a diffusion of the implanted atoms, or of oxygen, or of both species. Moreover in the case of boride films the overlap of B(d, p_0) and O(d, p_1) reactions hampered an accurate determination of the O content in wear tracks (the less intense O(d, p_0) emission was used). SIMS analysis were very valuable because nearly quantitative profiles of B (and C) could be recorded when using Cs^+ ions as sputtering particles: in such analytical conditions the SIMS signals were not sensitive to the chemical environment of atoms [21]. But when a target is sputtered with ions of a noble gas (Ar^+ in our experiments) secondary ion yields can be multiplied by more than a thousand if oxygen is adsorbed or implanted in the surface [17, 22–26]. This chemical effect was used to investigate the oxidation process of films during friction (dissolution of oxygen in the bulk of films or in the substrate through cracks).

3. Experimental results

3.1. Structure of as-implanted films

The results of *in situ* experiments on Ti foils implanted with N, B are detailed in [14, 15]. The structural changes observed successively for increasing fluences of N were:

1. The development of radiation damage.
2. The precipitation of the ε-Ti_2N nitride (quadratic structure described in [27] in epitaxy with the Ti matrix, and the collapse of precipitates into a continuous film.
3. Precipitation of the δ-TiN cubic nitride, also in epitaxy with Ti and Ti_2N. The identification of this latter confirmed our previous data by X-ray diffraction at grazing incidence on bulk specimens, in opposition to other TEM studies [11–12].

Similarly B implantations did not lead to amorphization nor to the precipitation of TiB_2 as in previous investigations on bulk samples implanted at high current density (and perhaps with some contamination) [8, 16]. TiB precipitates were identified for

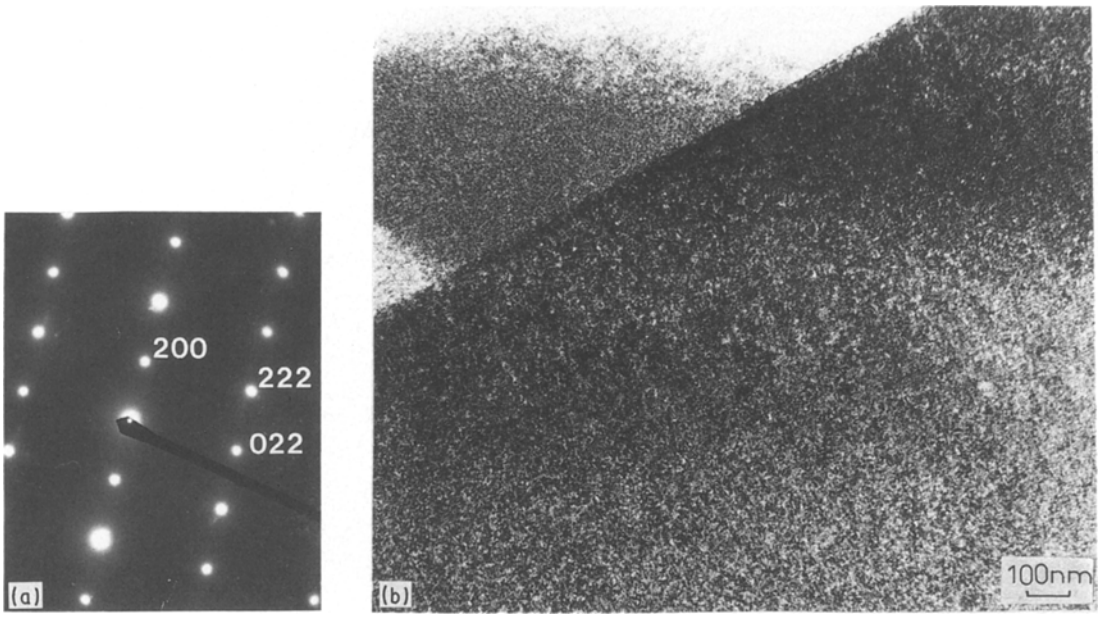

Figure 3 T.E.M. observations of titanium implanted with 10% N and 10% O (same film as in Fig. 1); (a) diffractogram, (b) dark field.

implanted contents over 1%, in agreement with the phase diagram. There was not a single epitaxy relationship between these precipitates and a given Ti grain contrary to Ti_2N or TiN. Indeed the three lattice parameters of TiB [25–30] are multiple integers of the Ti ones, and at least a dozen of planes containing a [1 0 0], [0 1 0] or [0 0 1] direction were found to grow parallel to basic, prismatic or pyramidal planes of Ti. Thus the continuous TiB film obtained for 40 to 60% B exhibited only a texture.

In the case of nitrides a simple epitaxy between planes of close packing, i.e. {0 1 0} in Ti_2N, {1 1 1} in TiN and (0 0 0 1) in Ti, is preferred because the directions of close packing (respectively [1 0 1], [1 1 0] and [1 1 $\bar{2}$ 0]) form an angle of 60° in the three phases and the distance between Ti atoms along these directions is the same to within 2%. Note however that part of the TiN grains were randomly oriented (diffraction rings superimposed to the single crystal sections) contrarily to Ti_2N ones.

The structure of other compounds which were identified in bulk samples implanted at five energies are summarized in Table I. In all crystalline phases formed in pure Ti, the small grains exhibited a perfect coherency within domains corresponding to a former grain of the matrix. Their nature could thus be cross-checked by tilting the foil and recording at least three single crystal sections on each area forming an angle equal to the tilt. If samples implanted with 40 to 50% C or N+O had of course the same fcc structure than TiN, a new compound was observed in Ti implanted with 10% N + 10% O. Its quadratic structure of the $\varepsilon - Ti_2N$ type (antirutile) is proven without ambiguity by the diffractogram of Fig. 3, which cannot be indexed as a section of a cubic lattic. Vardiman [31] suggested that such compounds with a complex structure would form in implanted metals because the array of metal atoms remains unchanged during the transformation. On the contrary the stacking order of close packing planes is different in TiN and Ti.

Ti_2AlN coatings could never be prepared by PVD or CVD processes [32]. Thus it appeared interesting to obtain this phase by ion implantation of N in Ti_2Al, even if tribological tests could not be performed

TABLE I Nature of formed compounds, epitaxies with the substrate and approximate hardness normalized to the TI one (2.5 GPa)

System	Compound	Epitaxies	H/H_{Ti}*
Ti + N	Ti_2N quadratic	{0 1 0}, {1 1 1}//(0 0 0 1)	15 ± 5
	TiN fcc	{1 1 1}//(0 0 0 1)	30 ± 10
Ti + C	TiC fcc	{1 1 1}//(0 0 0 1)	17 ± 7

Ti + B	TiB orthorhombic	(0 0 1), (1 1 0), (1 1 1), (1 0 2), (2 1 1)//(0 0 0 1)
		(0 1 0), (0 1 1), (1 0 2)//(0 1 1 0)
		(1 1 1)//(0 1 1 1)
			8 ± 3

Ti + N + O	$Ti_2(N, O)$ quadratic	ibid. Ti_2N	20 ± 10
	Ti(N, O) fcc	ibid. TiN	22 ± 10

Ti_2Al + N	Ti_2AlN hp8	(0 0 0 1)//(2 0 $\bar{2}$ 1) + (1 0 $\bar{1}$ 1)//(0 2 $\bar{2}$ 1)
		(1 0 $\bar{1}$ 2)//(1 0 $\bar{1}$ 0)
		(1 0 $\bar{1}$ 3)//(0 0 0 1) or (1 1 $\bar{2}$ 0)	

	Ti_2AlN_3 fcc		
TiAl + N	$TiAlN_2$ fcc	ibid. TiN	20 ± 10
TiAl + C	$TiAlC_2$ fcc	ibid. TiN	17 ± 3
TiAl + B	amorphous boride		5 ± 1

*Error bars on hardness values correspond to depth gradients measured with a same indentor. Despite the uncertainty on the real hardness of each film, the mean values of H/H_{Ti} are representative of the difference in the hardness of films.

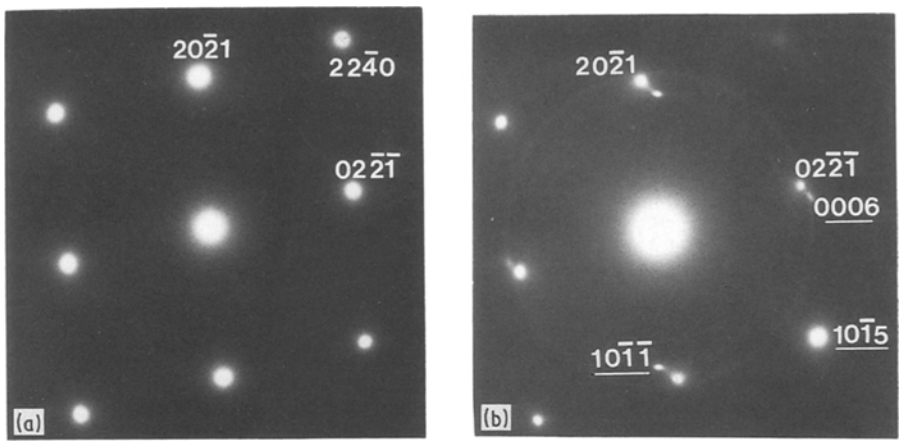

Figure 4 Diffractograms recorded on a Ti_2Al thin foil implanted *in situ* with increasing fluences of 50 keV N^+ ions: (a) before implantation, (b) 2×10^{16} N^+, (c) 10^{17} N^+ cm^{-2}.

afterwards on the specimens. Diffraction patterns recorded *in situ* during implantation attested the precipitation of this compound for implanted concentrations over 1%. Figs 4a and b show for instance the $[3\,\bar{3}\,0\,2]$ section of Ti_2Al recorded before implantation and the superimposed $[\bar{1}\,2\,\bar{1}\,0]$ section of Ti_2AlN appearing after implantation of 2×10^{16} to 10^{17} N^+ of 50 keV per cm^2. $\{2\,0\,0\}$ and $\{1\,1\,1\}$ planes of Ti_2AlN_3 (fcc phase identical to δ-TiN), which have spacings comparable to $(0\,0\,0\,6)$ and $\{1\,0\,\bar{1}\,1\}$ in Ti_2AlN, would give rise to reflections at 54° instead of 80°. The fcc nitride precipitated at higher fluences, as evidenced by the pattern of Fig. 4c recorded on the same area. Despite the likeness of Ti_2AlN and Ti_2Al hexagonal lattices (hp8 and hp6 respectively with a basal parameter two times larger for the alloy) [30, 32] a simple epitaxy was not found. The nitride grains nucleated such that any plane with a low index and containing one $\langle 1\,0\,\bar{1}\,0\rangle$ direction (i.e. $(0\,0\,0\,1)$ but also $\{1\,0\,\bar{1}\,X\}$ with X = 1, 2, 3) was parallel to one of the basal, pyramidal or prismatic planes of the alloy ($(0\,0\,0\,1)$, $\{1\,0\,\bar{1}\,0\}$, $\{1\,1\,\bar{2}\,0\}$ or $\{2\,0\,\bar{2}\,1\}$), which contain also $\langle 1\,0\,\bar{1}\,0\rangle$ or $\langle 1\,1\,\bar{2}\,0\rangle$ directions. On the contrary $\{1\,1\,1\}$ or $\{1\,1\,2\}$ planes of δ-Ti_2AlN_3 were always in epitaxy with $\{2\,0\,\bar{2}\,1\}$ planes of Ti_2Al.

This fact explains that the nitride or carbide grains in films containing 40 to 50% C or N (implantations in bulk specimens) exhibited an as perfect coherency within each former Ti_2Al grain as Ti_2N grains in Ti. On the contrary, diffractograms recorded on TiAl implanted with 50% C or N were superimposed sections of the fcc δ-$TiAlC_2$ or δ-$TiAlN_2$ lattice. This difference might be due to the fact that TiAl has a fcc structure of the AuCu type, with a different stacking order of close packing planes with respect to Ti [30] while the Ti_2Al lattice is only a substructure of the Ti one.

The formation of an amorphous boride in TiAl implanted with 40 to 50% B, instead of an orthorhombic monoboride as in Ti, is also understandable. Indeed the only known compound in the ternary phase diagram (not well established) is $TiAlB_4$ isomorphous of TiB_2 and AlB_2 [35].

All types of compounds exhibited a very fine grain (in the range 10 to 20 nm) (Fig. 3b) like most single phased films obtained by ion implantation. Indeed the nucleation of a new phase generally results from statistical fluctuations of the composition induced by collision cascades and the nucleation rate becomes very large as the implanted concentration exceeds a threshold value. On the contrary the growth rate is more dependent on the long range diffusion of implanted atoms, since a depleted zone forms around each nucleus.

3.2. Friction and wear

The results described below deal with friction tests against steel except when stated in the text. Two types of friction curves have been recorded, either continuous recordings of the friction coefficient along a close circuit (rectangular) during 2000 cycles, or recordings at the end of wear tests along one of the line composing the scan.

In both types of tests, no significant difference has been observed between the various compounds formed in Ti for implanted concentrations over 20%. Their initial friction coefficient against steel was in all cases of (0.25 ± 0.05) instead of (0.35 ± 0.10) for pure Ti. In some cases it exhibited a transcient increase up to 0.6 during running in, then stabilized at a value

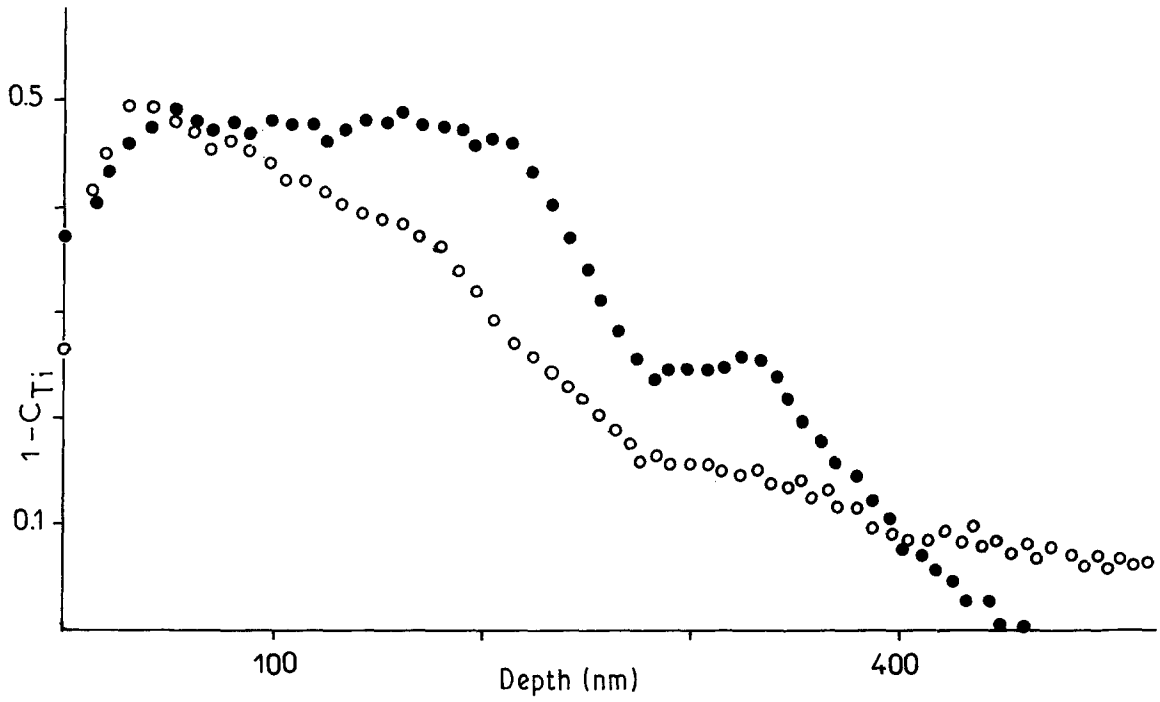

Figure 5 Depth profiles of ($1\text{-}C_{Ti}$)obtained by an iterative processing of the R.B.S. spectra in Ti–50% ^{14}N (●) as annealed 4 h at 600° C, (○) after 500 scans under a pressure of 0.7 GPa. The first one is identical to the N profile (10^{17} O cm^{-2} against $2\,10^{18}$ N), while the second one is the profile of O diffusion during friction (less than 10^{16} N cm^{-2} measured by N.R.A.). The spectrum recorded on the unworn surface was also fitted by means of a simulation program with 2 layers of 210 nm TiN and 115 nm Ti_2N.

of (0.4 ± 0.1), while in other cases it increased slowly up to this value. But this behaviour was not correlated, nor to the composition of the film, nor to the contact pressure. After prolonged tests leading to a removal of the film from more than 10% of the implanted area (crushing process of wear detailed below), it increased again up to (0.8 ± 0.2). Stick and slip events were then easily perceptible because of the low speed chosen for the tests (0.5 mm sec^{-1}). They can be associated to adhesion between bare areas of Ti and steel. The high value of the mean coefficient is also due to the transfer of hard particles of the film on the rider (observed by SEM). Indeed the friction coefficient of pure Ti or of a Ti–10% N α-solid solution under pressures up to 0.3 GPa was only of (0.35 ± 0.2), and that of a TiO_2 anodic film (0.20 ± 0.05).

The amount of wear after 100, 250, 500 or 2000 scans under increasing pressures was assessed on basis of tracks analysis by means of RBS, NRA and SIMS (for B) since the worn depth remained always lower than the tracks roughness (scars and plastic deformation) until complete removal of the implantation films. The amounts of B, N, C, O per unit area in as-implanted surfaces and wear tracks are summarized in Table II. Their variations with the pressure and the length of the test indicate clearly that the kinetics of wear depends critically on the contact pressure. This one can be compared to estimations of the flow stresses of films and substrates, taken equal to the tensile strength (0.5 GPa for Ti) or a third of the hardness (Table I) [36]. The hardness of implantation films was measured by means of a submicroscopic indentation test, but with large uncertainties due to bluntings or contaminations of the diamond or to the lack of a real hardness plateau for hard and elastic compounds [37].

Under a macroscopic pressure of 0.1 GPa, a Ti–10% N film (α-solid solution) exhibited a good wear resistance, but it was worn after less than 100 scans when the pressure was increased up to 0.3 GPa. A TiO_2 anodic film or a sputtered BN coating on Ti (with thicknesses about 200 nm in both cases) were worn after the same number of scans but under the lowest pressure of 0.1 GPa. On the contrary, a ε-Ti_2N film containing 20 to 25% N could undergo 2000 scans under 0.3 GPa or even 500 scans under 0.8 GPa without significant wear. Under this last pressure, a film with the same cristallographic structure but containing 10% N and 10% O was completely worn after less than 200 scans. Ti 50% N and 10% O films were only slightly more resistant, as also Ti–50% N films contaminated with oxygen during implantation, which were always worn after 500 scans. One of these δ-Ti 50% N film has also been annealed 4 h at 600° C in order to coarsen the nitride grain and suppress stresses in film and substrate. After this thermal treatment, it exhibited a duplex structure constituted by superimposed TiN and Ti_2N layers (Fig. 5), because solute N atoms and Ti_2N precipitates already present in less implanted regions of the as-implanted sample (evidenced by X-ray diffraction at grazing incidence [13]) collapsed into a continuous layer. The presence of a Ti_2N underlayer did not improve the lifetime of the film with respect to an as implanted specimen because of a further contamination during the annealing treatment. The dissolution of oxygen in the δ phase seems to affect critically its hardness (Table I) and wear resistance. Indeed pure Ti–45% N films could undergo tests of 1000 scans under the same pressure.

It is not possible to compare quantitatively the wear resistances of TiB, TiC and TiN on the basis of the few tests performed until now. For each number of scans

TABLE II

Composition matrix metalloid %			Wear parameters		Measured amounts of implanted atoms		Contaminants $\times 10^{16}$ cm^{-2}		
			Gpa	Scans	Initial dose $\times 10^{16}$ cm^{-2}	Residual fraction	^{16}O	^{12}C	Fe
		0	0	0	0		4 ± 1	2 ± 1	0
			0.1	20			10	5	1
			0.1	100			20	2	1
			0.1	500			58	17	7
			0.3	500			50	2	0
			0.7	500			45	2	0
		10 ± 1	0	0	23 + 5	1	4 ± 1	1	0
			0.1	500		0.9 ± 0.1	80 ± 20	12 ± 3	7 ± 1
			0.3	500		0.1 ± 0.1	70 ± 20	2 ± 1	0
			0.7	500		0.1 ± 0.1	60 ± 10	2 ± 1	0
		24 ± 2	0	0	60 + 10	1	6 ± 1	2 ± 1	0
			0.1	500		1	12 ± 2	4 ± 1	2 ± 1
Ti	N		0.3	500		0.8 ± 1	12 ± 1	3 ± 1	3 ± 1
			0.3	2000		0.8	10	3	5 ± 1
			0.7	500		0.8 ± 2	80 ± 40	10 ± 3	5 ± 1
			0.7	1000		0	/	/	0
			1.2	50		0.1	50	2	0
			1.2	250 RUBY		1	30	/	0
			1.2	1000 RUBY		0.5	90	/	0
		45 ± 5	0	0	150 + 10	1	6 ± 1	2 ± 1	0
			0.1	500		0.8	7	3	1
			0.7	100		1	/	/	0
			0.7	500		0.8 ± 0.1	40	2	3
			0.7	1000		0.4	35		10
			1.2	100		0	/	/	0
			1.2	1000 RUBY		0.8	/	/	0
		50 ± 5	0	0	210 + 10	1	12	2	0
			0.3	500		1	30 ± 5	4 ± 1	3 + 1
			0.3	2000		0.9 ± 0.1	60 ± 10	6 ± 1	7 + 2
			0.7	100		1	20	5	2
			0.7	500		0	40 ± 10	3 ± 1	0
ANNEALED			0	0		1	12	10	0
			0.7	500		0	80	10	0
		10 ± 10	0		24 ± 24	1	4	1	0
	N		0.7	250		0	70	2	0
	+	50 ± 10	0	0	170 ± 25	1	15 (± 25)	3	0
	O		0.3	1000		1	25 (± 25)	5	4
			0.7	500		0	50 ± 10	2 + 1	0
	C	40 ± 2	0	0	140	1	9	/	0
			0.7	250		0.8	80	/	7
			0.7	500		1	40	/	10
			0.7	1000		0.4	/	/	/
			1.2	250		0	70	/	0
			1.2	1000 RUBY		0.7			
			1.2	2000 RUBY		0	/	/	0
	B	40 ± 2	0	0	170	1	8	1	0
			0.7	500		0.9 ± 1	50 ± 20	/	10
			0.7	1000		1	/	/	13
			0.7	2000		0.8	/	/	/
			1.2	1000 RUBY		0.5	45	/	0
TiAl	C	40 ± 2	0	0	140	1	8	/	0
			0.7	500		1	8	/	0
			1.2	500		1	10	/	0
			0.1	500 TIN		1	9	/	0
			0.1	1000 TIN		0.7	8	/	0
			0.1	2000 TIN		0	11	/	0
	B	39 ± 1	0	0	175	1	17	4	0
			0.7	500		1	19	2	0
			0.1	500 TIN		0.3	100	4	0
			0.1	1000 TIN		0	40	4	0
	N	41 ± 1	0	0	140	1	7	3	0
			0.1	500 TIN		1	10	/	0
			0.1	1000 TIN		0.6	12	/	0
			0.1	2000 TIN		0.6	15	/	0

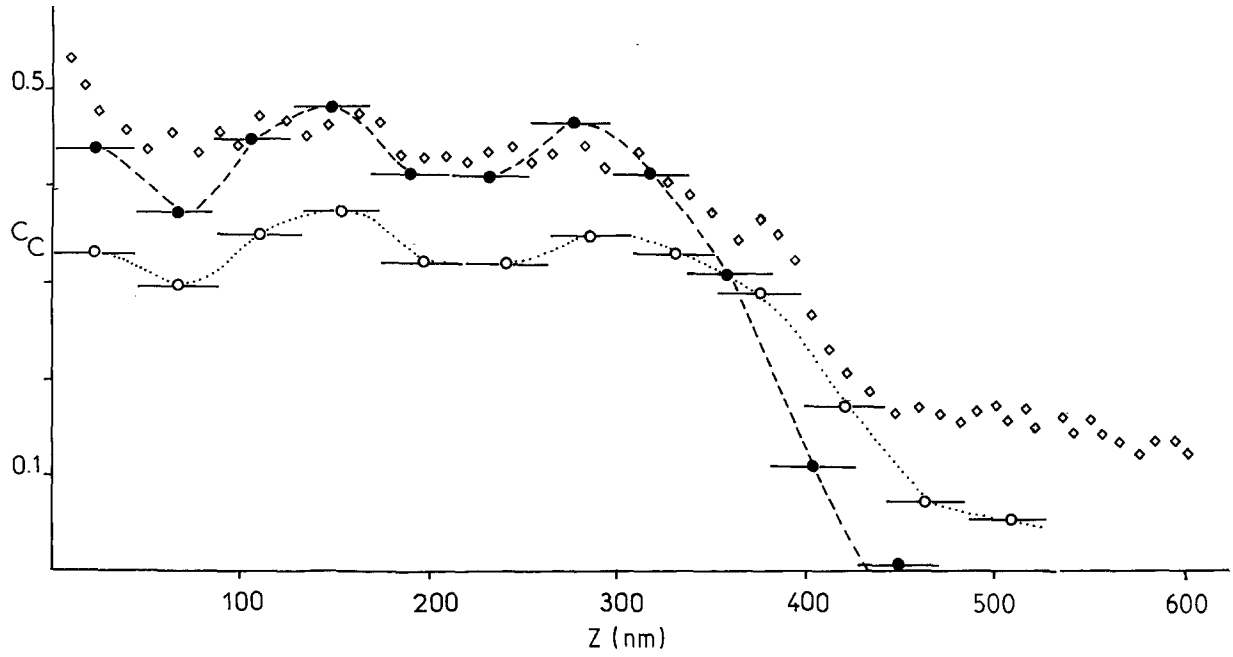

Figure 6 RBS profiles of ^{12}C atoms using 5.7 MeV He^+ ions in (●) Ti as implanted with 1.4×10^{18} C cm^{-2}, (○) after 250 scans under a pressure of 0.7 GPa (residual dose = 1.0×10^{18} C cm^{-2}). Horizontal bars correspond to the thicknes of layers with a given composition introduced in the simulation of RBS spectra to fit the experimental ones. (◇) RBS profile of $(1 - C_{Ti})$ using 2 MeV He^+.

at least ten tests would be necessary to give a statistical significance to plots of the wear kinetics. Indeed, if each track was homogeneously worn (this fact was checked by recording several SIMS profiles), the wear rate was not reproducible for a given length of the test. The acceleration of the crushing kinetics depended aleatorily on transfer and adhesion events. However one can state that TiB was a little more resistant than the carbide or the nitrides. For instance it could undergo more than 300 scans under a pressure of 1.2 GPa instead of less than 100 scans for TiN and TiC and 50 scans for Ti_2N. The two cubic TiC and TiN phases exhibited comparable resistances (under 0.7 and 1.2 GPa). An inverse order was observed in tests with ruby balls. But a more interesting result is the increase of more than a factor 5 in the performance of all compounds when rubbed against ruby instead of steel, for an identical diameter of the riders ("Hertzian" pressure of 1.2 GPa), despite the higher hardness of ruby.

The difference between the Vickers hardnesses of studied Ti and TiAl substrates was not very large: (2.5 ± 0.1) GPa for Ti and (3.2 ± 0.3) GPa for TiAl. This low hardness of the TiAl alloy (with respect for instance to a TiAl12%V4% alloy: 5 GPa) could be due to its (1 1 1) texture. However its wear resistance under a pressure of 0.7 GPa was estimated to be about 10 times the Ti one, on basis of three-dimensional recordings of wear tracks. Each type of compound (B, C or N) exhibited also a comparable hardness whatever its substrate (Table I). But all implantation films on the alloy were much more resistant than those on pure Ti since no significant loss in the implanted fluence nor change in the N, C or B depth profiles have been detected after 500 scans of steel or ruby balls under pressures of 0.7 or 1.2 GPa. Their friction coefficient against steel was also a little lower and more constant: (0.18 ± 0.02). They could only be abraded with TiN balls of radius 1 cm. Despite a lower value of the macroscopic pressure, such tests were more severe because of the hardness and of the surface roughness of these riders. In such conditions the boride exhibited the highest abrasion kinetics and the nitride was the most resistant (Table II).

3.3. Composition and structure of worn films

The results of RBS, NRA, SIMS and XPS analysis of wear tracks in Ti, TiAl6%V4% implanted with N are detailed in [16, 34]. The surfaces of pure Ti or Ti–N solid solutions (Ti–10% N) oxidized during friction, whatever the pressure of contact. A film of iron hydroxide was also built on the rider surface and in part transferred onto the Ti counterpart, accounting for the increasing amount of Fe atoms (measured by RBS, Table II) with the number of scans under low contact pressures. SEM images and topography recordings made by means of a stylus technique evidenced that the wear mechanism was a mild abrasion of superficial oxide layers. When the contact pressure was increased, it changed into a severe adhesive wear, characterized by: (a) the topography of the track, and (b) the increasing fluctuations of the friction coefficient due to stick and slip events. The transferred particles of $Fe(OH)_x$ and TiO_2 ones were removed from the track (Table II) and accumulated at the end of lines scanned by the rider. NRA data and RBS or SIMS profiles showed also that, whatever the pressure and the extent of wear, oxygen diffused in Ti at depths exceeding 2 μm. A mean content of 10% O has been measured on this range of depth.

Oxygen diffused also through all implantation films formed in Ti as shown for instance by the RBS profiles of Figs 5 and 6. When concentration profiles of implanted atoms could be recorded separately by means of a resonant nuclear reaction or backscattering at higher energy (Fig. 6), their comparison with RBS

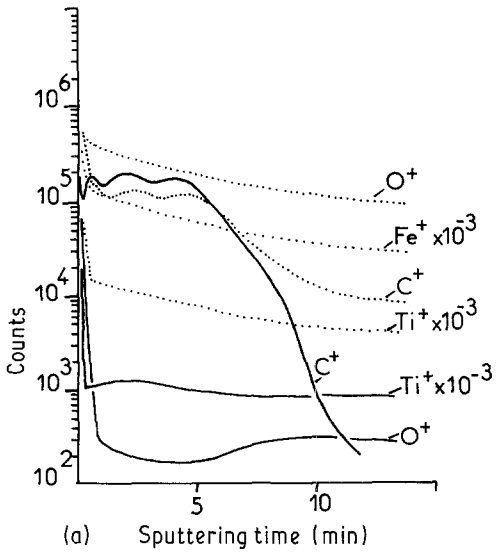

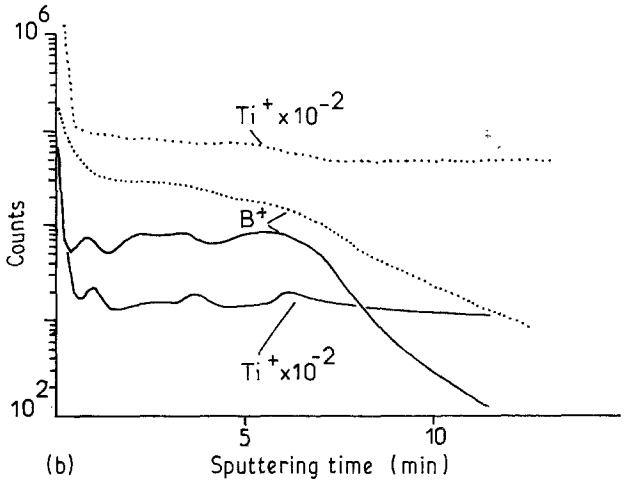

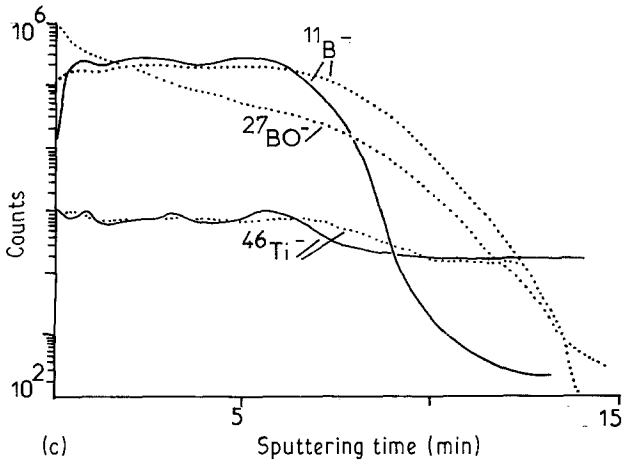

Figure 7 SIMS profiles recorded on TiC and TiB after friction tests of respectively 250 and 500 GPa against steel under a pressure of 0.7 GPa. (a) TiC analysed with an Ar^+ bombardment; (b) TiB in the same analytical conditions; (c) TiB analysed with a Cs^+ bombardment.

profiles of the Ti concentration allowed to see that:
– the shape of the C or N distribution did not change but part of the film was removed such that the C or N concentration per unit area (1 mm^2 investigated) decreased.
– there was a shallow gradient of oxygen diffusion into the substrate.

The abrasion process by local crushing of these various films, instead of a peeling layer by layer, is also demonstrated by the SIMS profile of Fig. 7a. The bumps of the C distribution are at the same depth in the wear track and in the as-implanted surface. The slight widening of C, B or N profiles recorded by SIMS are accounted by a differential sputtering of transferred or crushed particles, but the implanted element never diffused, like in steels. The fact that a noticeable oxidation was already detected before the films were worn does not imply necessarily that oxygen diffused in their lattice. In the case of δ–TiN or TiC films SIMS analysis rather indicated that it diffused through cracks. Indeed the intensity of secondary ions characteristic of the compound (N^+, C^+, TiN^+, TiC^+) decreased in the ratio of the wear amount measured by NRA or RBS while the intensity of ionic species emitted in part by the substrate (Ti^+) increased (Fig. 7a).

On the contrary Ti_2N films on Ti underwent a partial transformation into δ-Ti(N, O), as shown by the diffractograms and electron micrograph of Fig. 8. This oxidation occurred preferentially at the boundaries between blocks of Ti_2N grains with a common orientation (grown in epitaxy with a given Ti grain, Fig. 8b), and sometimes within one block. The (2 0 0) spot in the diffraction pattern (Fig. 8c) cannot be indexed as a Ti_2N or Ti pole: the nearest d_{hkl} differ of 10% {2 0 0} and {1 1 1} rings were also recorded on other areas. The tilt angle of 54° between diffractograms (Figs 8c and d) corresponds also to the angle between both Ti_2N and TiN sections. This oxidation was corroborated by experiments of X-ray diffraction at grazing incidence and by SIMS profiles. The insertion of oxygen atoms into the bulk of the nitride induced an enhancement of N^+, TiN^+-emissions [17].

A similar oxidation was shown for the boride TiB (Figs 7b and c). While the nearly quantitative B^- profile recorded under caesium bombardment shows that the film has not yet been worn, the B^+ emission measured under argon bombardment is strongly enhanced. The oxidized state of boron is confirmed by the BO^- profile recorded with caesium. Ionic images have also shown that the chemical enhancement of emissions was not restricted to areas in the vicinity of iron oxide grains.

Contrary to Ti, the unimplanted TiAl alloy was not oxidized during friction tests against steel, even under high contact pressures – neither diffusion nor thickness increase of the superficial oxide has been detected by SIMS. Similarly the carbide or nitride films were not contaminated with O or N of the TiN riders (Table II). A slight oxygen gradient over about 100 nm in the TiAl substrate was only recorded when about all the film had been worn, but a strong oxidation was put into evidence for the boride when rubbed with TiN. The B^+ SIMS emission measured under argon bombardment was multiplied by 100 when the film was already half worn.

4. Discussion and conclusions

The higher wear resistance of the TiAl substrate with respect to Ti in friction tests against steel cannot be

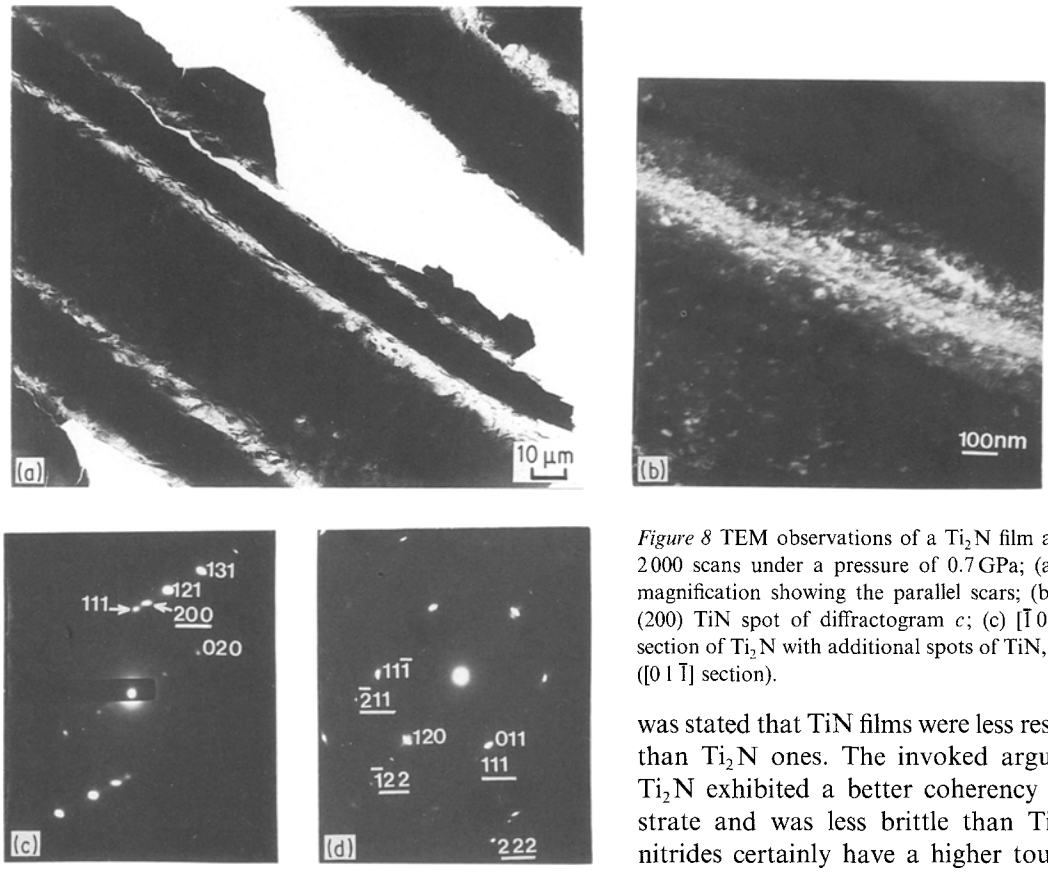

Figure 8 TEM observations of a Ti_2N film after a friction test of 2000 scans under a pressure of 0.7 GPa; (a) bright field at low magnification showing the parallel scars; (b) dark field with the (200) TiN spot of diffractogram *c*; (c) [$\bar{1}$ 0 1] section; (d) [2 $\bar{1}$ 1] section of Ti_2N with additional spots of TiN, which are underlined ([0 1 $\bar{1}$] section).

attributed to its hardness. It is rather due to its resistance to oxidation and seizure. Similarly each type of implantation compound had a hardness nearly independant of its substrate but it was less reactive when containing aluminium. Thus all implantation films on the TiAl alloy underwent only a mild abrasion. By contrast, the abrasion of films on Ti was accelerated as soon as they had been partially spalled by the tensile stress following adhesion events between Ti and the steel counterpart.

Previous experiments on the Ti Al 12% V 4% alloy implanted with N ions [34] have shown that, under the lowest pressure of tests presented in this paper (with the same steel riders but with a pin on disc rotational configuration) the friction coefficient of Ti_2N films began to increase sooner than in the case of TiN films. Both types of nitride films were not worn after 3000 revolutions, or after 3000 scans with the tribometer used here. But like implantation films on pure Ti, the Ti_2N ones oxidized during friction and more iron was transferred on their surface than on TiN. These facts and the evidence of the poor resistance of Ti(N, O) or Ti_2(N, O) under higher contact pressures, indicate that oxinitrides stick to the iron rider contrary to pure nitrides or carbides. The adhesion energy between oxinitrides and iron oxide is naturally strong, because of the ionic character of the chemical bond in both compounds, and it is lower for covalent carbides or nitrides. What is astonishing is that a contamination with only $6 \times 10^{16}\,O\,cm^{-2}$, i.e. a content ratio of 2% O/50% N, in the bulk of the nitride is sufficient to increase its wear kinetics by about a factor 5. Note here that such a contamination was not taken into account in two of our previous publications, where it was stated that TiN films were less resistant to abrasion than Ti_2N ones. The invoked arguments were that Ti_2N exhibited a better coherency with the Ti substrate and was less brittle than TiN. In fact both nitrides certainly have a higher toughness than oxinitrides because of their mixed covalent-metallic nature. The hardness of antirutile films measured by submicroscopic indentation was about half that of δ-TiN and two thirds that of δ-Ti(N,10% O). This could explain that the Ti_2N wear resistance was intermediate between the TiN and Ti(N, O) ones. Until its degree of tribo-oxidation attains a critical level the lower Ti_2N/Ti ratio of hardness and the higher toughness of the nitride provide a better resistance to spalling. As argued in our previous papers δ-Ti(N, O) films are too brittle to undergo the same deformation as their substrate when the contact pressure exceeds a given threshold. On the basis of the present tests this threshold would be about 0.3 GPa, i.e. the hardness of titanium.

On the other hand, the results of friction tests on Ti compounds with ruby, or on TiAl ones with TiN, are more relevant of their respective abrasion resistances since they do not depend on the adhesion between the metallic substrate and a steel rider. The cubic carbide and nitride exhibited comparable performances with a Ti substrate, and the nitride was a little more resistant than the carbide when on a TiAl substrate. An opposite result was obtained by Singer, but in abrasion tests with SiC powder [8], and it was shown here in comparative tests with riders of different natures that this last factor is of primordial importance. Despite the difference of their structures, TiB and TiAlB had both higher abrasion rates than carbides or nitrides. This result could be expected on the basis of their lower hardness. Their strong oxidation during friction most certainly is also a factor increasing their wear kinetics. One can consider, for example, the case of iron oxide films which lubricate the contact when they exhibit an optimal range of thickness but are pulled off when they are too thick [39, 40]. The chemical stability of

boride coatings is controversial [1, 5]. However in any friction conditions, against TiN, ruby or steel, a protective B_2O_3 layer did not develop on our implantation films. Similar experiments on TiB_2 films prepared either by ion implantation or ion beam mixing will be performed in the near future in order to compare their oxidation rate to the TiB, TiAlB ones.

Acknowledgements

Thanks are due to J. Perriere of Solid State Physics Group of ENS Paris, GDR 202, N. Moncoffre of IPN Lyon, G. Rotureau, G. Brault of ETCA, O. Kaitasov and J. Chaumont of CSNSM for their assistance in implantations and analysis.

References

1. H. HOLLECK, *J. Vac. Sci. Technol.* **A4** no. 6 (1986) 2661.
2. W. D. MÜNZ *J. Vac. Sci. Technol.* **A4** (1986) 2717.
3. J. W. JONES and J. WERT, *Wear* **32** (1975) 363.
4. J. L. SULLIVAN, T. F. J. QUINN and D. M. ROWSON, *Tribology International* **13** (1980) 153; *Wear* **65** (1980) 1; *Wear* **94** (1984) 175.
5. J. E. SUNDGREN and H. T. G. HENTZELL, *J. Vac. Sci. Technol.* **A4** no. 5 (1986) 2259.
6. R. MARTINELLA *et al.*, *Mat. Sci. Eng.* **69** (1985) 247.
7. R. N. BOLSTER, I. L. SINGER and R. G. VARDIMAN, *Surf. Coat. and Technol.* **33** (1987) 469.
8. I. L. SINGER *et al.*, *ibid.* (1988) p. 531.
9. R. G. VARDIMAN, in Materials Research Society Symposium Proceedings 27 (1984) (Elsevier, Sci. Pub.) p. 699.
10. W. C. OLIVER *et al.*, Materials Research Society Symposium Proceedings **27** (1984) p. 705.
11. D. FLECHE, J. P. GAUTHIER and P. KAPSA, *J. Microsc. Spectrosc. Electron.* **10** (1985) 219.
12. R. HUTCHINGS, *Mater. Sci. Eng.* **69** (1985) 129.
13. J. C. PIVIN *et al.*, *J. Mater. Sci.* **22** (1987) 1087.
14. P. ZHENG and J. C. PIVIN, *M. O. Ruault, Europhys. Lett.* **8** no. 6 (1988) 689.
15. J. C. PIVIN and P. ZHENG, *M. O. Ruault, Phil. Mag. Lett.* **59** no. 1 (1989) p. 25.
16. S. OKAMOTO *et al.*, *J. Amer. Ceram. Soc.* **66** (1983) C78.
17. J. C. PIVIN, *Surf. Interf. Anal.* **13** (1988) 37.
18. A. CHEVARIER *et al.*, *Trace and Microprobe Techniques* **6** (1988) 1.
19. E. LIGEON and A. BONTEMPS, *J. Radioanal. Chem.* **12** (1972) 335.
20. M. O. RUAULT, J. CHAUMONT and H. BERNAS, *Nucl. Instrum. Methods* 209–210 (1983) 351; *IEEE Trans. Nucl. Sci.* **20** (1983) 1746.
21. G. BRAULT *et al.*, to be published in *Surf. Interf. Anal.*
22. G. SLODZIAN, in SIMS III Proceedings, edited by A. Benninghoven, J. Giber, J. Laszlo, M. Riedel, H. M. Werner (Springer Series in Chemical Physics, Springer, Berlin, Heidelberg, New York) **19** (1982) 115.
23. J. C. PIVIN, C. ROQUES-CARMES and G. SLODZIAN, *Int. J. Mass. Spectrosc. Ion Phys.* **31** (1979) 293 and 311.
24. *Idem, ibid.* **26** (1978) 219.
25. *Idem, J. Appl. Phys.* **51** (1980) 4158.
26. *Idem, J. Microsc. Spectrosc. Electron.* **7** (1982) 277.
27. B. HOLMBERG, *Acta Chemica Scan.* **16** (1962) 1255.
28. DECKER, *Acta Crystallogr.* **7** (1954) 77.
29. KUGAI, *Inorganique Material,* (English Translations) **8** (1972) 669.
30. W. B. PEARSON, P. VILLARS and L. D. CALVERT, in "Pearson's Handbook of Crystallographic Data for Intermetallic Phases", (American Soc. for Metals Pub. 1985, Ohio).
31. R. G. VARDIMAN, in "Ion Implantation 1988", edited by F. H. Wohlbier, Defect and Diffusion Forum 57–58 (Trans Tech Pub Suisse.31). Marca (1988) 135–142; marca, *Met. Trans.* **2** (1971) 465.
32. O. KNOTEK, H. BOHMER and T. LEYENDECKER, *J. Vac. Sci. Technol.* **A4** no. 6 (1986) 2695.
33. ENCE, *J. of Metals* **9** (1961) 484.
34. J. C. SCHUSTER and J. BAUER, *J. Solid State Chem.* **53** (1984) 260.
35. MARCA, *Met. Trans.* **2** (1971) 465.
36. H. M. POLLOCK, unpublished work.
37. J. D. J. ROSS *et al.*, *Thin Solid Films* **148** (1987) 171.
38. J. C. PIVIN *et al.*, submitted to *J. Phys. D.*
39. F. PONS, J. C. PIVIN and G. FARGES, *J. Mater. Res.* **2** no. 5 (1987) 580.
40. Y. MIZUTANI, in "Fundamentals of Tribology", edited by N. P. Suh and N. Saka (MIT Press, Cambridge, 1980) pp. 223–236.
41. J. L. SULLIVAN, in "Tribology – Fifty Years On" (Institution of Mechanical Engineers, London, 1987).

Received 7 February
and accepted 24 August 1989